

# On dynamic and thermodynamic components of cloud changes

Sandrine Bony, Jean-Louis Dufresne, Hervé Le Treut

Laboratoire de Météorologie Dynamique du CNRS

Paris, France

Jean-Jacques Morcrette

European Center for Medium Range Weather Forecasts

Reading, England

Catherine Senior

Hadley Center, Meteorological Office

Bracknell, England

Climate Dynamics

Revised manuscript, August 2003

Corresponding author:

Dr Sandrine Bony, LMD, boîte 99, 4, place Jussieu, 75252 Paris cedex 05, France.

e-mail: [bony@lmd.jussieu.fr](mailto:bony@lmd.jussieu.fr) ; tel: +33 (0)1 44 27 50 14 ; fax: +33 (0)1 44 27 62 72

## Abstract

Clouds are sensitive to changes in both the large-scale circulation and the thermodynamic structure of the atmosphere. In the Tropics, temperature changes that occur on seasonal to decadal timescales are often associated with circulation changes. Therefore, it is difficult to determine the part of cloud variations that results from a change in the dynamics from the part that may result from the temperature change itself. This study proposes a simple framework to unravel the dynamic and non-dynamic (referred to as thermodynamic) components of the cloud response to climate variations.

It is used to analyze the contrasted response, to a prescribed ocean warming, of the tropically-averaged cloud radiative forcing (CRF) simulated by the ECMWF, LMD and UKMO climate models. In each model, the dynamic component largely dominates the CRF response at the regional scale, but this is the thermodynamic component that explains most of the average CRF response to the imposed perturbation. It is shown that this component strongly depends on the behaviour of the low-level clouds that occur in regions of moderate subsidence (e.g. in the trade wind regions). These clouds exhibit a moderate sensitivity to temperature changes, but this is mostly their huge statistical weight that explains their large influence on the tropical radiation budget.

Several propositions are made for assessing the sensitivity of clouds to changes in temperature and in large-scale motions using satellite observations and meteorological analyses on the one hand, and mesoscale models on the other hand.

# 1 Introduction

The temperature of the Tropics constitutes an essential boundary condition for the extratropical climate. Its regulation plays thus a key role in the regulation of the global climate (e.g. Pierrehumbert 1995). It has long been suggested that tropical temperatures have not varied much during the past thousand years, despite significant variations of the atmospheric concentration in greenhouse gases and solar forcing (CLIMAP 1981). Although this evidence is now brought into question (Yin and Battisti 2001 and references herein), several studies using simple climate models have investigated the mechanisms whereby the tropical ocean-atmosphere system could get rid of an external radiative perturbation and get regulated. Among these mechanisms, a change in the relative area of subsiding and ascending branches of the large-scale atmospheric circulation has been pointed out as an efficient way to modify the longwave cooling to space and thereby limit the surface temperature change induced by an external perturbation (Pierrehumbert 1995). On the other hand, it has been emphasized that the sensitivity of cloud properties to a change in surface temperature or in the thermodynamic structure of the atmosphere could significantly affect the tropical energy budget and hence constitute a powerful feedback mechanism (e.g. Miller 1997, Larson et al. 1999, Lindzen et al. 2001). On a theoretical basis, it thus recognized that radiative feedback processes may be composed of dynamic and thermodynamic components. This applies in particular to cloud radiative feedbacks: the change in the radiative impact of clouds induced directly or indirectly by an external perturbation may result partly from a change in the large-scale atmospheric circulation, and partly from a change in the thermodynamic structure of the atmosphere.

The radiative impact of clouds, that is usually referred to as the cloud radiative forcing (CRF), and the tropical Earth's radiation budget critically depend on the type of clouds (Dhuria and Kyle 1990, Hartmann and Michelsen 1992). As illustrated on Figure 1, this latter is controlled to a large extent by the large-scale atmospheric circulation: large-scale atmospheric subsidence favors the formation of low-level boundary layer clouds (stratus, strato-cumulus) while large-scale ascending motions associated with convective activity produce cumuliform clouds ranging from shallow to deep and extensive clouds. Owing to this dynamic control, shifts or local variations of the CRF often reflects shifts or variations

in large-scale circulation patterns. This has been well documented in the case of spatio-temporal variations (Hartmann and Michelsen 1993, Bony et al. 1997, Klein and Jakob 1999, Norris and Weaver 2001) and in the case of El-Niño climate variations (Allan et al. 2002, Chen et al. 2002). On the other hand, some studies point out that clouds can be intrinsically sensitive to a change in the thermodynamic structure of the atmosphere. For instance, Klein and Hartmann (1993) suggest that the stratus cloud amount decreases as the surface temperature increases, likely because of the effect of surface temperature changes on the low-level static stability. Recently, Del Genio and Kovari (2002) suggest that the precipitation efficiency of clouds in convective systems increases with temperature. Yet, the intrinsic sensitivity of clouds to temperature has not been much documented so far. A fundamental reason is that the large-scale atmospheric circulation is thermally forced in the Tropics. Variations in the circulation are thus often associated with temperature variations, and it is not straightforward to unravel the part of cloud variations that results from changes in the dynamics from the part that results from an intrinsic temperature dependence. As a result, the interpretation of cloud variations in observations or in numerical simulations is not always straightforward.

Ramanathan and Collins (1991) pointed out a strong correlation between CRF and sea surface temperature (SST) variations over warm tropical oceans, that was interpreted as a thermodynamic mechanism of regulation of ocean warming by cirrus clouds. It was subsequently shown that this correlation reflects mostly the control of clouds and CRF by the large-scale atmospheric dynamics rather than a fundamental dependence on temperature (Hartmann and Michelsen 1993, Bony et al. 1997). Recently, a large decadal variation of radiative fluxes in the Tropics has been observed (Wielicki et al. 2002). This variation seems related to a strengthening of the Hadley-Walker circulations over the last two decades (Chen et al. 2002). Allan and Slingo (2002) show that a mode reminiscent of ENSO (El-Niño Southern Oscillation) variability and associated with strong dynamical shifts explains about 45% of the total decadal variation. Dynamic effects thus control a significant part of the decadal variation of clouds and radiative fluxes. However, higher-order modes of the decadal variation are more difficult to interpret. They may be related to dynamic effects associated with other modes of natural variability, or to non-dynamic effects. Indeed, the last two decades have been associated with a significant warming of the ocean temperature

(Levitus et al. 2000). Part of the decadal variation of clouds may thus reveal the intrinsic sensitivity of clouds to temperature changes. Making more explicit the relative roles of dynamic and non-dynamic effects in this variation would help clarifying this issue.

On the modeling side, the interpretation of the cloud response to climate perturbations is not much easier. It is well recognized that climate models produce cloud radiative feedbacks (i.e. changes in CRF in response to an external perturbation) that differ greatly among the models (Le Treut and McAvaney 2000). Even for a given model, their sign may differ according to the type of climate perturbation considered. For instance, Del Genio et al. (1996) show that the CRF anomaly produced by the Goddard Institute for Space Studies (GISS) GCM is positive in response to a uniform SST perturbation, while it is negative when the longitudinal SST gradient over the Pacific is altered. More recently, Yao and Del Genio (2002) show that cloud radiative feedbacks produced by the GISS model are significantly different for climate changes associated with different patterns of SST change. As the modification of the tropical atmospheric circulation closely depends on the pattern of SST change, one may speculate that these results reflect differences in the dynamic component of the cloud response.

We argue that unraveling the dynamic and thermodynamic components of the cloud response to a climate perturbation would help *(i)* to interpret the cloud or radiation variations that are observed on long timescales in the current climate, *(ii)* to understand the diversity of cloud radiative feedbacks produced by climate models, and *(iii)* to design strategies of evaluation of GCM clouds and radiation than would allow to put constraints on the climate sensitivity simulated by the models.

In section 2, we propose a simple methodology to unravel and to quantify the dynamic and thermodynamic components of cloud and radiation changes in observations or in models. In section 3, we use this method to analyze the contrasted responses of three GCMs regarding the sensitivity of the tropical CRF to a prescribed climate warming. The relative roles of dynamic and thermodynamic components at the regional scale and at the tropic-wide scale are discussed, and the factors that control the magnitude of each component on the large scale are pointed out. Based on these results we propose, in section 4, a strategy for evaluating the dynamic and thermodynamic components of the modelled cloud response to climate change using satellite observations or mesoscale models. A summary

and a conclusion are given in section 5.

## 2 Framework of analysis

### 2.1 Method

To unravel the dynamic and thermodynamic components of cloud variations, we attempt to make more explicit the link between clouds and the large-scale atmospheric circulation. Let  $C$  be any cloud or radiative variable (such as cloud fraction, CRF, cloud water content or radiative flux), and  $\omega$  a proxy of the large-scale atmospheric circulation. Since the cloud types and CRF are strongly controlled, at first order, by the large-scale vertical motion of the atmosphere, here we use the large-scale vertical velocity at 500 hPa (expressed in hPa/day) for  $\omega$ . Then, we discretize the large-scale tropical (30°S-30°N) circulation onto a series of dynamical regimes corresponding to different values of  $\omega$  (intervals of 10 hPa/day are used to define the circulation regimes). So doing, the ascending branches of the Hadley-Walker circulation, that occur mostly over the warmest portions of the Tropics, correspond to negative values of  $\omega$ , while regions of large-scale subsidence correspond to positive values of  $\omega$ . The statistical weight of each dynamical regime over the Tropics, defined as the area covered by regions having a vertical velocity  $\omega$  normalized by the total area of the Tropics, is referred to as  $P_\omega$ . As any Probability Distribution Function (PDF),  $P_\omega$  verifies:

$$\int_{-\infty}^{+\infty} P_\omega d\omega = 1 \quad (1)$$

Owing to mass conservation constraints, the tropically-averaged vertical motion defined as  $\int_{-\infty}^{+\infty} \omega P_\omega d\omega$  is close to zero.

Let  $\bar{C}$  refer to the tropically-averaged value of  $C$ . Classically, it may be defined as  $\bar{C} = \sum_i \sigma_i C_i / \sum_i \sigma_i$  where  $i$  refers to an individual region or a model gridbox of the Tropics,  $\sigma_i$  to the area of this region,  $C_i$  to the value of  $C$  in this region, and the sum over  $i$  refers to all regions of the latitude belt comprised within  $\pm 30^\circ$  of latitude. Alternatively, if  $C_\omega$  refers to the mean value of  $C$  in the dynamical regime defined by  $\omega$  (in practice,  $C_\omega$  is computed by compositing the regional values of  $C$  in  $\omega$  bins of 10 hPa/day<sup>1</sup>),  $\bar{C}$  can be expressed in

---

<sup>1</sup>Although we use, in practice, finite intervals of  $\omega$  of 10 hPa/day to define dynamical regimes, we will consider in the following notations that  $\omega$  intervals are infinitesimal.

the " $\omega$  basis" as:

$$\bar{C} = \int_{-\infty}^{+\infty} P_{\omega} C_{\omega} d\omega \quad (2)$$

We now consider climate perturbations around a time-mean state (that may correspond to a long-term average of climate variables or, in numerical experiments, to a "control" climate). Let  $\delta C$  refer to the temporal perturbation of  $C$  around its time-averaged value. The tropically-averaged change in  $C$  associated with a climate change may be expressed as<sup>2</sup>:

$$\overline{\delta C} = \int_{-\infty}^{+\infty} C_{\omega} \delta P_{\omega} d\omega + \int_{-\infty}^{+\infty} P_{\omega} \delta C_{\omega} d\omega + \int_{-\infty}^{+\infty} \delta P_{\omega} \delta C_{\omega} d\omega \quad (3)$$

The first rhs term of the above equation arises from changes in the large-scale atmospheric circulation associated with the climate change. Those may be horizontal shifts of the large-scale dynamical patterns, or local changes in the intensity or in the sign of the large-scale vertical motion. It will be referred to as the *dynamic* component of  $\overline{\delta C}$ . The second term arises from the change of cloud or radiative properties under given dynamical conditions. As it represents the part of  $\overline{\delta C}$  that does not directly result from circulation changes, it will be referred to as the *thermodynamic* component of the  $C$  response to climate change. It may arise for instance from the intrinsic sensitivity of  $C$  to temperature variations, and eventually from other processes such as changes in the atmospheric composition or indirect effects of aerosols. The last term arises from the correlation of dynamic and non-dynamic effects in  $\overline{\delta C}$ . We will refer to it as the term of *co-variation*<sup>3</sup>.

## 2.2 Illustration

To illustrate the approach, we use monthly mean data of 500 hPa large-scale vertical velocities derived from meteorological reanalyses and CRF data derived from the satellite Earth's Radiation Budget Experiment (ERBE, Barkstrom 1984). Here, these data are

---

<sup>2</sup>The discretized form of this equation, that is used in practice here, is of the form:  $\overline{\delta C} = \sum_{\omega} C_{\omega} \Delta P_{\omega} + \sum_{\omega} P_{\omega} \Delta C_{\omega} + \sum_{\omega} \Delta P_{\omega} \Delta C_{\omega}$  where  $\Delta C_{\omega}$  and  $\Delta P_{\omega}$  refer to the changes in  $C_{\omega}$  and  $P_{\omega}$ .

<sup>3</sup>The change in cloudiness that occurs in a particular region of the Tropics may result from both local and remote influences. At first approximation, if one considers that the remote effects are felt by clouds mostly through changes in the large-scale atmospheric motion, then the changes in cloud properties that occur for a given dynamical regime (the so-called thermodynamic component) can be considered as being much less dependent on remote effects. We insist however that this is only an approximation: remote effects may affect clouds through other factors than a change in  $\omega$  (a change in the temperature lapse rate, the occurrence of dry intrusions in the mid troposphere, etc).

used over the period 1987-88, at a spatial resolution of  $2.5^\circ \times 2.5^\circ$ . Following Coakley and Baldwin (1984), the longwave and shortwave components of the CRF are defined as:  $C_{LW} = LW_{clear} - LW$  and  $C_{SW} = SW - SW_{clear}$ , where  $LW$ ,  $SW$ ,  $LW_{clear}$  and  $SW_{clear}$  refer to as the outgoing longwave radiation (OLR) and the absorbed shortwave radiation at the top of the atmosphere (TOA) in actual and clear-sky conditions, respectively. Since the vertical velocity is not directly assimilated, it may be influenced by the GCMs used in the data assimilation system. This is particularly true over tropical oceans which are data void regions. To estimate the range of uncertainties in  $\omega_{500}$  that may be associated with model biases, we use three independent sets of meteorological reanalysis: the European Centre for Medium-Range Weather Forecasts Atmospheric Reanalysis (ERA, Gibson et al. 1997), the reanalysis produced at the National Centers for Environmental Prediction in collaboration with the National Center for Atmospheric Research (NCEP/NCAR, Kalnay et al. 1996), and that produced at the Data Assimilation Office of the National Aeronautics and Space Administration (NASA/DAO, Schubert et al. 1993). Figure 2 shows the PDF of  $\omega_{500}$  and the mean relationship between  $C_{LW}$  and  $\omega_{500}$  over the Tropics ( $30^\circ\text{S} - 30^\circ\text{N}$ ) that is derived from the combined use of ERBE data and of meteorological reanalyses.

$P_\omega$  is negatively skewed and presents a strong maximum for  $\omega_{500}$  around 10-20 hPa/day. This distribution can be explained from simple physical considerations. The rate of subsidence of the free tropospheric air is primarily constrained by the clear-sky radiative cooling rate of the atmosphere. Ch eruy and Chevallier (2000) show that in the Tropics, the clear-sky longwave heating rate is about -2 K/day with a standard deviation of about 0.5 K/day. For  $\partial\theta/\partial z = 5$  K/km, this corresponds to a large-scale vertical velocity of 15-20 hPa/day (a few mm/s). The pick in  $P_\omega$  thus reveals the large area of the Tropics that is associated with a clear-sky free troposphere. Such regions are found mostly in the subtropics and over the eastern part of the ocean basins, often in coincidence with the presence of low-level clouds in the boundary layer. The positive tail of  $P_\omega$  presumably corresponds to the regions where the upper troposphere is the driest and the longwave radiative cooling the strongest.  $P_\omega$  is much smoother in regimes of large-scale ascent. Since ascending motions occur nearly entirely within cumulus clouds and since the rate of subsidence of air in-between clouds is constrained by the clear-sky radiative cooling, the magnitude of the large-scale vertical velocity reflects the magnitude of vertical motions within clouds. The magnitude of  $\omega$  for

$\omega < 0$  is thus related to the vigor of the convective mass flux. Note that in such a framework, the tropical warm pool appears as the negative tail of  $P_\omega$ .

The OLR primarily reflects the temperature at the emission level of infrared radiation. In cloudy conditions, this reflects the altitude of the cloud top: the higher the cloud top, the smaller the OLR at the top of the atmosphere and the larger the LW CRF. Low values of  $C_{LW}$  observed for positive values of  $\omega_{500}$  reflect thus the presence of low-level boundary layer clouds in subsidence regimes. The fact that  $C_{LW}$  does not vary much with  $\omega_{500}$  in subsidence regions shows that in these regions the height of cloud tops does not depend much on the strength of the sinking motion. On the contrary, the gradual increase of  $C_{LW}$  toward negative  $\omega_{500}$  reflects the increase in upper tropospheric cloudiness and the higher penetration depth of convective clouds as the convective activity intensifies.

### 2.3 Dynamic and thermodynamic components of radiative feedbacks

The tropically-averaged LW CRF,  $\overline{C_{lw}}$ , is the product of  $P_\omega$  and  $C_\omega$  summed over all circulation regimes (equation 2). A change in  $\overline{C_{lw}}$  may result from a change in the large-scale atmospheric circulation ( $\delta P_\omega$ ) without any change in cloud properties (dynamic component illustrated on Figure 2 by an horizontal arrow), or from a change in cloud properties ( $\delta C_\omega$ ) without any change in the statistical distribution of large-scale atmospheric motions (thermodynamic component schematized by a vertical arrow), or from both (equation 3).

The dynamic component ( $\int_{-\infty}^{+\infty} C_\omega \delta P_\omega d\omega$ ), may be associated with a change in the fractional area covered by large-scale ascending motions ( $\int_{-\infty}^0 P_\omega d\omega$  vs  $\int_0^{+\infty} P_\omega d\omega$ ) or, more generally, by a change in the statistical weight associated with the individual dynamical regimes. Circulation changes ( $\delta P_\omega$ ) associated with a climate perturbation are hardly predictable at the regional scale, because they depend on the details of changes in surface temperature patterns and thus on the nature of the perturbation and on the timescale. However, the "cloudy dependence" of the dynamic component ( $C_\omega$ ) may be assessed from available data. This will be discussed in more detail in section 4. The thermodynamic component ( $\int_{-\infty}^{+\infty} P_\omega \delta C_\omega d\omega$ ) arises from cloud changes within individual dynamical regimes. The contribution of a particular regime to this component depends on both the magnitude of cloud changes ( $\delta C_\omega$ ) and the statistical weight  $P_\omega$  that this regime represents in the Tropics.

As stressed by Pierrehumbert (1995), it is necessary to consider the energy budget of the whole Tropics to understand the response of the tropical climate to an external perturbation. This applies in particular to the understanding of cloud radiative feedbacks. Yet, the investigation of cloud feedbacks in observations, in simple models or in GCMs has often focussed on the role of deep convective clouds on the one hand, and on that of stratus clouds on the other hand (e.g. Larson et al. 1999, Lindzen et al. 2001). The former occur in regions of intense convective activity and the latter in regions of strongest static stability and subsidence strength (Klein and Hartmann 1993, Norris 1998, Bony et al. 2000). These dynamical regimes correspond mostly to the tails of  $P_\omega$ :  $\int_{-\infty}^{-40} P_\omega dw$  and  $\int_{30}^{+\infty} P_\omega dw$  each represent roughly 10% of the Tropics (not shown). With that regard, these regimes can be considered as extreme. The rest of the Tropics (about 80%), that is associated with comparatively more moderate values of  $\omega$ , is covered by ubiquitous low-level cumulus clouds (Norris 1998). Hartmann and Michelsen (1992) showed that on a global average basis, low clouds make the largest contribution to the net energy balance of the Earth. Here, we stress that the role of low-level cumulus clouds in tropical cloud radiative feedbacks is presumably essential.

In the following, we use the above framework to analyse the response of the CRF simulated by three GCMs to an imposed uniform warming of the global ocean. Such a type of climate perturbation is not thought to be an excellent proxy of climate changes associated with an increased atmospheric concentration in greenhouse gases or with a change in the orbital parameters of the Earth: first, it does not involve any feedback between the atmosphere and the ocean and second, actual climate changes are generally associated with changes in the SST patterns of the Tropics, and thus with a substantial modification of the large-scale tropical circulation. Nevertheless, we will show that even for such a type of climate perturbation, unravelling the dynamic and thermodynamic components of the cloud response helps to point out the factors that primarily control this response in GCMs, and provides some guidance for proposing strategies of evaluation of these factors in GCMs that should be relevant for other types of climate change.

## 3 Analysis of climate change experiments

### 3.1 Models and experiments

We analyze idealized simulations from three atmospheric GCMs: (1) the ECMWF GCM, a version of the ECMWF spectral model run in a climatic mode at a resolution of T63 and 31 levels in the vertical with a non-operational physical package, (2) the LMD GCM, the version 2.0 of the grid-point LMDZ model run at a resolution of 3.75 by 2.5 degrees and 19 sigma levels in the vertical, and (3) the UKMO GCM, which is the HadAM3 version of the GCM developed at the Hadley Center, run at a resolution of 3.75 by 2.5 degrees with 38 vertical levels. These three models were forced with daily SSTs and run over a period of 18 months from May 1987 to October 1988, as part of a European Community funded project on cloud feedbacks and validation. A detailed description of the ECMWF and LMD models together with a careful assessment, using ISCCP and ERBE data and a model-to-satellite approach, of the cloudiness produced in their simulations are presented in Webb et al. (2001). The HadAM3 version of the UKMO model is described in Pope et al. (2000), and its cloudiness is evaluated in Williams et al. (2003) by using techniques similar to those used by Webb et al. (2001). In this study, we compare the sensitivity of the ECMWF, LMD and UKMO models to a prescribed ocean warming. For this purpose, another set of simulation is performed by each model, in which the SST is uniformly increased by 2 K. Beside the SST, all other forcings and parameters of the models are unchanged.

### 3.2 Overview of model results

The tropically-averaged change in CRF induced by the 2 K warming of the global ocean turns out to be very contrasted among the three GCMs:  $-1.8 \text{ W/m}^2$  for the ECMWF GCM,  $+0.85 \text{ W/m}^2$  for the LMD GCM, and  $+2.0 \text{ W/m}^2$  for the UKMO GCM (Table 1). Such contrasts among GCMs (both in sign and in magnitude) remain when considering only tropical oceans (not shown), and when considering global changes: the globally-averaged change in CRF in these experiments is  $-2.4 \text{ W/m}^2$ ,  $+0.5 \text{ W/m}^2$  and  $+0.82 \text{ W/m}^2$  for the ECMWF, LMD and UKMO GCMs, respectively. Since the Tropics represent roughly 50% of the Earth's area, a simple calculation shows that in the LMD and UKMO GCMs, the Tropics dominate the global CRF response, while the Tropics and the extratropics contribute

more equally in the ECMWF model.

As shown by Figure 3, the regional response of the LW and SW CRF (defined as the monthly  $C'_i - C_i$  where  $i$  refers to a model grid box and  $C_i$  and  $C'_i$  to the monthly CRF values in this grid box in the Control and in the +2K experiment, respectively) to a uniform change of SST is far from uniform. The positive and negative patterns of CRF anomalies may reveal different intrinsic sensitivities of clouds to the SST change, or the influence of regional circulation changes. Visual examination suggests that large CRF variations are often associated with significant changes in  $\omega_{500}$ . This is confirmed by figure 4 showing that on average, and despite the large standard deviations that reflect the diversity of factors contributing to regional cloud forcing variations, the magnitude of regional (or local) LW or SW CRF anomalies ( $C'_i - C_i$ ) scales almost linearly with that of  $\omega_{500}$  anomalies ( $\omega'_i - \omega_i$ ). Moreover, the regional change in CRF that occurs when there is no monthly circulation change ( $\Delta\omega_i = 0$ ) is very weak compared to regional CRF changes that occur in the presence of circulation changes. The regional response of clouds or CRF to a global climate perturbation appears therefore to be dominated by the circulation changes that occur at that (regional) scale<sup>4</sup>. However, the weakness of tropically-averaged changes in  $C_{LW}$  and  $C_{SW}$  (Table 1) shows that CRF changes associated with circulation variations are subject to substantial compensations among the Tropics.

Equation 3 allows to estimate explicitly the part of  $\overline{\delta CRF}$  that results from dynamic changes (the so-called dynamic component), and the part that is not dynamically forced (the thermodynamic component). Table 2 shows that the co-variation term of equation 3 is very weak; we can thus analyze the tropically-averaged change in CRF by focusing on dynamic and thermodynamic components. Both  $\overline{\delta CRF_{LW}}$  and  $\overline{\delta CRF_{SW}}$  turn out to be dominated by the thermodynamic component. Moreover, as the LW and SW dynamic components are of opposite sign,  $\overline{\delta CRF_{NET}}$  is even more dominated by thermodynamic changes than its individual components. The CRF response to the global SST perturbation is thus mostly dynamically forced at the regional scale, and thermodynamically forced at the Tropics-wide scale.

We note nevertheless that in the case of the LW cloud forcing, the magnitude of the dynamic component relative to that of the thermodynamic component is less negligible

---

<sup>4</sup>Note that the change in  $\omega$  that occurs in a given region results from both local and remote influences.

than in the case of the SW or NET cloud forcing, and it is negative in all three models. This can be understood by looking at tropical circulation changes between the CTRL and +2K experiments. The shape of  $P_\omega$  in the CTRL experiment somewhat varies among GCMs (Figure 5), especially the width of the peak in subsiding regions. Since the 500 hPa vertical velocity of subsiding air is mostly constrained by the clear-sky radiative cooling of the free troposphere (section 2), these differences probably reveal differences in the simulation of the upper tropospheric cooling rate. This latter depends on the upper tropospheric humidity (UTH) prediction, as well as on the radiation code used to predict its radiative impact. The fundamental source of UTH in subsidence regions is the large-scale advection of water vapor from convective regions (Salathe and Hartmann 1997, Pierrehumbert and Roca 1998). The UTH and then the clear-sky radiative cooling in the upper troposphere of subsidence regions is thus controlled by a combination of dynamical and microphysical processes (Emanuel and Pierrehumbert 1995). The representation of these processes, in particular the convective moistening, is generally poorly evaluated or constrained in GCMs (see Emanuel and Zivkovic-Rothmann 1999 for a discussion of that matter). The differences in  $P_\omega$  among the models may thus indirectly reveal differences in the simulation of water vapor in the upper tropical atmosphere. However, the change in  $P_\omega$  between the CTRL and +2K experiments is qualitatively more similar among the models: the change in  $P_\omega$ , which is largest where  $P_\omega$  is largest, shows that the uniform SST warming is associated with a decreased frequency of strong convective regimes and strong subsidence regimes, and with an increased occurrence of regimes of moderate subsidence. This reveals a weakening of the large-scale tropical circulation. This variation is consistent with the findings of the idealized numerical study of Larson and Hartmann (2002). Owing to the weak values of the LW cloud forcing in subsidence regimes (this was shown on Figure 2 for the observations and will be shown in section 4 for the models), this is mostly the change of  $P_\omega$  in the convective regimes that affects the tropically-averaged LW cloud forcing. Indeed, this is in the models where the occurrence of strong convective situations ( $\omega < -40 \text{ hPa/day}$ ) decreases the most (in the ECMWF and UKMO models), that the dynamic component of  $\overline{\delta CRF_{LW}}$  is the most negative.

In these experiments, however, the diversity of the global CRF responses among GCMs results primarily from different thermodynamic sensitivities of clouds to the 2 K warming.

In comparison, differences in the response of the large-scale circulation to the SST change or in the control of clouds by dynamical changes play secondary roles. The relative weakness of the dynamic component on the tropic-wide scale certainly results in part from the fact that the prescribed ocean warming is spatially uniform in these experiments (note nevertheless that the land-sea temperature contrasts change). The actual climate response to an external perturbation is likely to be associated with a change in the SST distribution and then with a larger change in the atmospheric circulation. The relative magnitude of the dynamic and thermodynamic components is thus certainly perturbation and timescale dependent. Therefore, the important issue associated with this decomposition lies mostly in the understanding and in the evaluation of the factors that control the sign and the magnitude of each component in GCMs.

### 3.3 Analysis of the thermodynamic component

We now analyze the thermodynamic component of the tropically-averaged change in CRF to determine some of the factors that control it and to interpret further the origin of differences among GCMs.

For each experiment (Control or +2K), we compute  $C_\omega$  using the  $C$  and  $\omega_{500}$  fields from that experiment. The difference between the perturbed and control values of  $C_\omega$  is referred to as  $\delta C_\omega$ . Figure 6 indicates that for each GCM, the largest changes in CRF ( $\delta C_\omega$ ) occur in deep convective regimes ( $\omega < -50$  hPa/day) and strong subsidence regimes ( $\omega > 40$  hPa/day). In deep convective regimes, the ECMWF and LMD GCMs exhibit a strengthening of both the LW and SW CRF in response to the +2K SST perturbation. As the LW and SW CRF are of opposite sign, the change in NET CRF is much weaker than the change in individual LW or SW components. In these two models, however, the strengthening of the SW CRF slightly exceeds that of the LW CRF and thus the net cooling effect of clouds occurring in deep convective regimes gets enhanced in the warmer climate. In the UKMO GCM, on the other hand, the LW CRF increases while the SW CRF decreases (note that since the SW CRF is negative, a decrease corresponds to a positive anomaly of the radiation budget TOA). This leads to a strong positive anomaly of the NET CRF, that corresponds to a reduced cooling of clouds. In subsidence regimes, the change in NET CRF simulated by each GCM is dominated by the change in SW CRF. In the LMD and UKMO GCMs, the

SW CRF (i.e. the albedo effect of clouds) is weakened in the warmer climate, leading to a positive anomaly of the NET CRF. The ECMWF exhibits the opposite behaviour.

The impact of these CRF changes upon the tropically-averaged CRF is computed by weighting these changes by the statistical weight of the dynamical regime in which they occur ( $P_\omega \delta C_\omega$ ). As discussed earlier, the shape of  $P_\omega$  somewhat varies among GCMs, but every model reproduces the main features of  $P_\omega$  that were revealed by the reanalyses (Figure 2), in particular the huge statistical weight of the regimes of moderate subsidence ( $0 < \omega < 40$  hPa/day) and the comparatively much lesser weight of extreme dynamical regimes. Due to this robust feature of the tropical atmospheric circulation, the contribution of the different dynamical regimes to the tropically-averaged CRF is not in proportion of the magnitude of CRF changes that occur in these regimes.

In each GCM, the largest contribution to  $\overline{\delta C_{NET}}$  comes from the regimes of moderate subsidence (bottom panel of Figure 6). This is mostly owing to the large statistical weight of these regimes, rather than to a large sensitivity of the CRF. In comparison, the contribution of CRF changes that occur in extreme dynamical conditions such as over the warm pool or regions of strongest static stability contribute much less to  $\overline{\delta C_{NET}}$ . As a first approximation, the sign of  $\overline{\delta C_{NET}}$  as well as the rank of GCMs is given by the change in CRF that occurs for  $0 < \omega < 30$  hPa/day. We note nevertheless that despite their weak statistical weight in the Tropics, deep convective regimes contribute significantly to the tropically-averaged change in CRF in the UKMO GCM, owing to the non-cancellation of the LW and SW variations of the CRF in this model.

This analysis illustrates the advantage of looking at cloud changes in specified dynamical regimes instead of simply looking at geographical maps: on the one hand, it makes it possible to minimize the role of dynamical effects in cloud changes, and thus to better point up other potential influences (e.g. that of temperature changes). On the other hand, it makes it easier to assess the relative contribution of different tropical areas (e.g. warm pools, anticyclonic regions) to Tropics-wide changes.

## 4 A proposal for the evaluation of climate models

By analyzing the properties of clouds in specified regimes of the large-scale circulation ( $C_\omega$ ), the link between the cloudiness and the large-scale circulation in the Tropics becomes more explicit. As discussed in section 3, this facilitates the interpretation of changes in the tropically-averaged cloudiness and radiation fluxes. In this section, we discuss the benefits of such an analysis for the evaluation of clouds and radiation in climate models.

### 4.1 Observational assessment of cloud properties in dynamical regimes

Owing to the strong influence of the large-scale dynamics on clouds, the comparison with observations of simulated distributions of cloud-related variables often reveals, at first order, discrepancies in the simulation of the circulation patterns (spatial shifts, wrong intensities). Therefore, a deficient simulation of clouds over a particular region is not necessarily due to a wrong behaviour of cloud parameterizations over this region; it may be caused by a deficient simulation of the regional circulation patterns, owing to a wrong behaviour of the parameterizations over remote regions. Comparing the observed and modelled cloud properties in specified circulation regimes allows to assess the simulation of clouds whatever the biases of their geographical distribution.

Figure 7 assesses the LW, SW and NET CRF simulated by the ECMWF, LMD and UKMO GCMs in different dynamical regimes (any other variable may be evaluated the same way). Observational estimates were derived using monthly CRF data from ERBE and monthly 500 hPa vertical velocities extracted from either the ERA, NCEP/NCAR or NASA/DAO reanalysis. Except in the deepest convective regimes ( $\omega < 50$  hPa/day), the discrepancy between these three observational estimates, that gives a rough measure of the uncertainty associated with vertical velocity analyses, is generally less than  $5 \text{ W/m}^2$  (note that estimates using ERA and NCEP/NCAR are in close agreement over most circulation regimes). In convective regimes,  $C_{LW}$  is systematically underestimated by the models, the more intense the upward motions, the more underestimated the  $C_{LW}$ . These discrepancies likely reflect an underestimate of the upper level cloudiness by the models. However, part of them may arise also from biases in the simulation of the clear-sky OLR owing to biases in the water vapor profile or in the temperature lapse rate. In comparison, the simulated  $C_{SW}$  is in

better agreement with observations. As a result, the degree of cancellation between the LW and SW components of the CRF is badly reproduced by the models, and the net cooling effect of the cloudiness occurring in deep convective regions is significantly overestimated. At the tropic-wide scale, a consequence of these biases is that the radiative impact of a change in the large-scale atmospheric circulation induced by any type of perturbation will be biased. At the regional scale, a consequence will be that a change in  $\omega$  will be associated with a cloud forcing change of wrong magnitude. This leads to a wrong coupling between cloud and surface properties, which can be particularly problematic in coupled ocean-atmosphere versions of these models.

To interpret the origin of these model biases, other variables such as the cloud fraction, the cloud vertical distribution, water content and optical properties should be assessed in the same way. To assess cloud properties in a meaningful way, a model-to-satellite approach such as that proposed by Morcrette (1991) or Yu et al. (1996) is required. This approach consists in computing quantities that are consistent with what is seen from space, from the models' profiles of temperature, humidity and clouds. Webb et al. (2001) and Williams et al. (2003) used such a method to assess the cloudiness simulated in the ECMWF, LMD and UKMO models. Their results suggest that the underestimate of the simulated LW CRF in convective regimes (Figure 7) is related to biases in the prediction of the vertical distribution of clouds in these regimes, particularly an underestimate of mid-level clouds in the UKMO model, and an underestimate of mid and upper-level clouds in the ECMWF and LMD models. On the other hand, the right simulation of the SW CRF in these models probably results from error compensations between different cloud types (see Webb et al. 2001 for a discussion of that matter). Indeed, owing to the significant albedo effect of low, middle and upper-level clouds, such compensations occur more easily in the SW than in the LW.

## 4.2 Constraints on the dynamic component

Both dynamic and thermodynamic components are likely to be involved in climate changes and have therefore to be assessed in climate models. However, their relative magnitude is likely to depend on the nature and on the timescale of the climate perturbation. In the numerical experiments considered in this study, the thermodynamic component is the

primary contributor to the tropically-averaged change in CRF. However, one expects the dynamic component to play a more important role, relatively, in the case of climate variations associated with modifications of the surface temperature distribution and thus of the large-scale atmospheric circulation. This is presumably the case with seasonal and ENSO variations. This might be the case also for paleoclimatic variations characterized by large changes in the distribution of insolation, orography or continents. Moreover, the dynamics can undergo large variations on the short-term and/or at short spatial scales. At these scales, and as illustrated by the present study (section 3), circulation changes are thus likely to be responsible for a large part of cloud variations. For all these reasons, it is equally important to evaluate the dynamic and thermodynamic components of cloud changes.

The circulation changes associated with a given climate perturbation are hardly predictable at the regional scale, and  $\delta P_\omega$  is difficult to evaluate. However, from the definition of the dynamic component ( $\int C_\omega \delta P_\omega dw$ ), we see that the term of the dynamic component *that depends on the simulation of clouds* is  $C_\omega$ . An accurate simulation of  $C_\omega$  guarantees therefore that the impact of circulation changes ( $\delta P_\omega$ ) on the tropically-averaged C will be properly simulated. By comparing the observed and simulated  $C_\omega$  (Figure 7, based on the current climate), one may thus put some constraints on the simulation of the dynamic component by climate models.

Although  $\omega_{500}$  constitutes a meaningful proxy of the large-scale tropical circulation, it is certainly simplistic or naive to consider that the response of clouds to a change in the dynamics is fully characterized by their response to a change in  $\omega_{500}$ . While the smoothness of  $C_\omega$  suggests that  $\omega_{500}$  constitutes an adequate "scaling factor" of the convective activity and of cloud properties, it does not represent obviously all the dynamical conditions that influence the development and the properties of clouds. Factors such as the vertical wind shear, the specific thermal stratifications associated with particular dynamical changes at the regional scale or the degree of organization of convective systems may also influence cloud properties at the regional scale, and can be variable for a given  $\omega$ . The evaluation and the improvement of cloud properties in specific dynamical regimes defined from  $\omega$  is thus only a first step in the evaluation of the dynamic component of cloud changes.

### 4.3 Constraints on the thermodynamic component

In comparison, the evaluation of the thermodynamic component of the cloud response to climate change is more challenging. The intrinsic sensitivity of cloud properties to temperature constitutes a potentially critical factor for the sign and the magnitude of the thermodynamic component. However, inferring this sensitivity from observations requires great caution, particularly in convective regions. First, the sensitivity of convective clouds to temperature is presumably much weaker and thus more difficult to observe than that to large-scale motions (Bony et al. 1997, Lau et al. 1997, Tompkins and Craig 1999, Wu and Moncrieff 1999). Second, temperature and circulation in convective regions often vary together at the monthly timescale. Figure 8 shows the mean relationship between the SST over tropical oceans and the 500 hPa vertical velocity derived from each GCM (related results from meteorological analyses are presented in Bony et al. 1997): while large-scale subsidence occurs over a wide range of SSTs (more than 8 degrees) with a relatively uniform strength, large-scale rising motions of different intensities occur over a narrow range of SST (only a few degrees), and the transition from large-scale subsidence to large-scale ascent is fairly discontinuous in terms of SST (around  $27^{\circ}\text{C}$  in the control climate). As suggested by Bony et al. (1997) and Lau et al. (1997) and as illustrated here by the relationship derived from the SST+2K simulations, the value of this SST "threshold" is not universal<sup>5</sup>. It depends on the tropically-averaged temperature and seems rather related to the distribution of the ascending branches of the Hadley-Walker circulation over the SST distribution: large-scale rising motions occur mostly over tropical regions that are warmer by one degree or more than the tropically averaged temperature (this could change if the vertical velocity of subsiding air were to change), their frequency of occurrence increasing with temperature except at very high temperatures (above  $29.5^{\circ}\text{C}$  in the control simulation and over  $31.5^{\circ}\text{C}$  in the SST+2K experiment)<sup>6</sup>. Figure 8 shows that on average, an SST variation of 1 K

---

<sup>5</sup>For the current climate, Sud et al. (1999) suggested these temperature thresholds to be constrained by the relationship between the vertical profiles of dry and moist static energy in the tropical atmosphere. Figure 8 suggests that the SST thresholds derived from this relationship might depend on the mean tropical temperature.

<sup>6</sup>The reason for the decrease of convective activity or large-scale convergence at very high temperatures, pointed out and characterized by Waliser and Graham (1993) and Waliser (1996), is still a matter of study: it has been proposed that it could be related to the subsidence induced by remote forcings such as the large-scale subsidence associated by intraseasonal waves over the warm pool (Bony et al. 1997, Lau et al.

in warm regions is associated with a large change in the frequency and in the intensity of large-scale motions<sup>7</sup> Although this average behaviour does not mean that in warm regions, spatio-temporal variations of the SST are *systematically* associated with variations of the large-scale ascent, it points to the fact that in these regions, it is unfrequent to observe temperature variations that are not associated with circulation changes. The analysis, in the current climate, of interannual variations of clouds and radiation over a long time period (several years) may nevertheless allow to derive significant statistics about the effect of temperature on cloud properties under specific dynamical conditions.

In subsidence regimes, another type of difficulty arises. The occurrence and the fractional cloud cover of boundary-layer clouds (the predominant type of cloudiness in these regimes) are highly sensitive to the low-level static stability of the atmosphere (Klein and Hartmann 1993). The spatial and seasonal variations of temperature being of much larger magnitude at the surface than in the free troposphere, the spatio-temporal variations of climate over a short-term period are presumably associated with large variations of the low-level static stability. In a global climate change or at the decadal timescale, on the contrary, the SST and the free tropospheric temperature vary more in concert, and are associated with weaker variations of the static stability. As far as boundary-layer clouds are concerned, spatio-temporal variations constitute therefore a poor proxy of global climate changes. Following Williams et al. (2003), interannual variations of clouds restricted to the months and the regions for which the monthly regional SST relative to the tropical average ( $SST - \overline{SST}$ ) is unchanged (which would guarantee that variations in static stability are weak) would constitute a better proxy of global climate changes.

#### 4.4 Idealized sensitivity experiments

As discussed above, inferring the sensitivity of clouds to temperature variations under a specified regime of circulation is not easy from observations. In that context, Cloud Resolving Models (CRMs) or Large Eddy Simulation (LES) models might constitute useful

---

1997), or by a positive feedback between tropical convection and water vapor (Tompkins 2001).

<sup>7</sup>Large-scale motions are sensitive to horizontal gradients in the boundary-layer entropy (Lindzen and Nigam 1987, Emanuel et al. 1994). The relationship between SST and boundary-layer entropy, and its link to the sharp increase of deep convection for SSTs above 26°C are discussed by Sud et al. (1999) and Folkins and Braun (2003).

tools for exploring the physical processes that control this sensitivity, and eventually for evaluating the sign of this sensitivity in climate models. Pioneer studies of this kind have been carried out by Lau et al. (1994), Tompkins and Craig (1999) and Wu and Moncrieff (1999).

Idealized numerical experiments may be designed to investigate with mesoscale and single column versions of GCMs (so-called SCMs) the sensitivity of cloud properties to a specified change in the large-scale vertical motion on the one hand, and to a change in the thermodynamical structure of the atmosphere on the other hand (Figure 9). A change in the large-scale vertical motion could be prescribed by specifying a vertical profile of large-scale vertical velocity in the atmosphere (idealized or derived from data), by using it to diagnose large-scale vertical tendencies of heat and moisture and then by using these tendencies as large-scale forcings of the model. A change in the thermodynamical structure of the atmosphere could be induced by specified change of the surface temperature, or by a change in the atmospheric concentration in carbon dioxide if the models predict the surface temperature using a land model or a slab ocean mixed layer. The comparison of CRM and SCM simulations run under consistent large-scale forcings, and the analysis of the physical processes that control the sensitivities of clouds in both kinds of models will contribute to the evaluation of the physical parameterizations used in climate models, and to the understanding of the physical processes that explain discrepancies among models. In particular, this study suggests that understanding what controls the sign of the sensitivity of cumulus clouds to a temperature change may be essential to assess and to improve the global climate sensitivity produced by climate models. International projects such as the GEWEX Cloud System Study (GCSS 1993) and the European Cloud Systems (EUROCS, <http://www.cnrm.meteo.fr/gcss/EUROCS/EUROCS.html>) have proved the relevance and the scientific interest of comparing and analysing simulations from mesoscale and climate models produced with consistent large-scale forcings.

Nevertheless, it is well known that the simulations from mesoscale models are sensitive to the parameterization of cloud microphysics that is used in these models (e.g. Wu et al. 1999, Grabowski 2003). This will presumably affect also the sensitivity of clouds to a change in temperature or in large-scale motion. In parallel to CRM/SCM intercomparisons, it will be therefore essential to assess the uncertainty of CRM results associated with the

representation of cloud microphysics, and to assess the sign and possibly the magnitude of CRM sensitivities from observational studies such as those proposed above.

## 5 Summary and conclusions

The cloud response to a climate change may be forced by large-scale circulation changes on the one hand, and by changes in the thermodynamic structure of the atmosphere on the other hand. This study proposes a simple analysis framework to unravel the dynamic and thermodynamic components of cloud changes in the Tropics. It is based on the decomposition of the large-scale atmospheric circulation into a series of dynamical regimes defined from the large-scale vertical velocity in the mid-troposphere, and on the compositing of cloud properties in the different circulation regimes. Such a framework, illustrated here by using satellite data of the cloud radiative forcing and different sets of meteorological reanalyses, may be used to analyze observed and simulated climate variations on different timescales. We hope in particular that this framework will be useful to analyze cloud and radiation variations that have been observed on interannual and decadal timescales (e.g. Wielicki et al. 2002, Chen et al. 2002), and will help to determine observationally the sign of the intrinsic sensitivity of clouds to temperature. In the current study, we use it to analyze, in three GCMs, the contrasted responses of the cloud radiative forcing to an idealized and prescribed perturbation (a uniform warming of the global ocean by the 2 K): the tropically-averaged change in CRF induced by the 2 K warming is -1.8, +0.85 and +2.0  $W/m^2$  for the ECMWF, LMD and UKMO models, respectively.

In each model, the regional change in CRF is primarily influenced by circulation changes. However, the tropically-averaged change is dominated by the thermodynamic component (i.e. the change in CRF that occurs within dynamical regimes). The contribution of a particular dynamical regime to this component is a compromise between the statistical weight of this regime in the Tropics, and the sensitivity of clouds to temperature in this regime. The largest sensitivities of the CRF to the temperature are found in regimes of deepest convection or strongest subsidence, but the contribution of these regimes to the tropic wide sensitivity is limited by the weak statistical weight of these regimes. On the other hand, low-level clouds occurring in regimes of moderate subsidence exhibit a weak

sensitivity to temperature changes, but greatly influence the tropically-average change in CRF owing to their huge statistical weight. The differences among the three models largely reflect differences in the sign and the magnitude of CRF changes that occur in regions of moderate subsidence, namely at the edge of warm pool regions and on the eastern side of the ocean basins.

The cloud response to an actual climate change is likely to involve both dynamic and thermodynamic components. However, the relative magnitude of the two components certainly depends on the spatial distribution and on the timescale of the climate perturbation. Each component has thus to be assessed in climate models. Some propositions are made for this purpose. This includes assessing the simulated cloud-related variables such as the cloud type, the cloud fraction, the cloud water content or cloud radiative properties (preferably diagnosed from a model-to-satellite approach) in specified regimes of the large-scale circulation, considering their mean value as well as their intrinsic sensitivity to temperature. Moreover, systematic comparisons between Cloud Resolving Models and Single Column Models may help investigating and assessing the physical processes that control the sensitivity of cloud properties to temperature on the one hand, and to large scale motion on the other hand. Assessing the sensitivity of simulated clouds to a change in large-scale motion or in temperature would help also to assess two-dimensional numerical experiments performed by climate models (Bretherton and Sobel 2002) or CRMs (Larson and Hartmann 2002) to investigate tropical radiative feedback processes involving interactions between clouds, radiation and the large-scale dynamics.

The results of this study emphasize the importance of assessing, in particular, the intrinsic sensitivity to temperature of clouds that occur in regions of moderate subsidence (e.g. the trade wind regions). Those constitute the overwhelming majority of the Tropics, and the three state-of-the-art GCMs considered here predict very different sensitivities for these clouds. Further studies are now required to investigate how these different sensitivities may relate to specific aspects of the physical parameterizations used in the models, such as the closure of shallow and deep convection schemes, or the way the cloud fraction and cloud water content are predicted in the models.

Simple climate models constitute unvaluable tools for investigating the physical processes that control the sensitivity of the tropical climate. Most of them represent the

tropical large-scale atmospheric circulation is a highly idealized way by considering one box of uniformly ascending motions and one box of uniformly descending motions (e.g. Pierrehumbert 1995, Miller 1997, Larson et al. 1999, Hartmann et al. 2001). Consistently, the description of cloud types and cloud optical properties in these models is also very idealized. For instance, one box is assumed to be covered by deep convective clouds and the other one by clear skies or stratus clouds. The effect and the relative role of cloud property changes and large-scale circulation changes in the tropically-averaged radiation budget may be affected by this idealization. For instance Fu et al. (2001) and Lin et al. (2002) showed that the sign of the cloud feedback associated with the iris hypothesis of Lindzen et al. (2001) is sensitive to the values that are given to cloud properties in each box of the model. We suggest that considering a more continuous and less simplistic description of the tropical circulation, such as that provided by  $P_\omega$ , would help better connections to be established between observations of the real climate and the representation of cloud properties in the model. This would probably decrease the sensitivity of model results to poorly-known input parameters to the model. We expect this would improve also the representation of low-level cumulus clouds that occur ubiquitously over the tropical oceans, in dynamical conditions that are generally less extreme than those found over the warm pools or over the strong anticyclonic regions on the eastern sides of the ocean basins. Hopefully, this would help to better determine the sensitivity of the tropical climate to an external perturbation.

## 6 Acknowledgements

This work benefited from discussions with Kerry Emanuel, Jean-Yves Grandpeix, Christian Jakob, Laurent Li, Mark Webb and Yun-Ichi Yano, and from comments of two anonymous reviewers. Part of this study was supported by the Environmental Program of the Commission of the European Communities (project ENV4-CT95-0126 entitled Cloud Feedbacks and Validation). French participants acknowledge the Programme National d'Etude Du Climat (PNEDC).

## References

- Allan, R. P. and Slingo, A. (2002). Can current climate model forcings explain the spatial and temporal signatures of decadal olr variations? *Geophys Res Lett*, 29: 101029–101032.
- Allan, R. P., Slingo, A., and Ringer, M. A. (2002). Influence of dynamics on the changes in tropical cloud radiative forcing during the 1998 El-Niño. *J Clim*, 15: 1979–1986.
- Barkstrom, B. R. (1984). The Earth Radiation Budget Experiment (ERBE). *Bull Am Meteorol Soc*, 65: 1170–1185.
- Bony, S., Collins, W. C., and Fillmore, D. (2000). Indian ocean low clouds during the winter monsoon. *J Clim*, 13: 2028–2043.
- Bony, S., Lau, K.-M., and Sud, Y. C. (1997). Sea surface temperature and large-scale circulation influences on tropical greenhouse effect and cloud radiative forcing. *J Clim*, 10: 2055–2077.
- Bretherton, C. S. and Sobel, A. H. (2002). A simple model of a convectively coupled Walker circulation using the weak temperature gradient approximation. *J Clim*, 15: 2907–2920.
- Chen, J., E, C. B., and Del Genio, A. D. (2002). Evidence for strengthening of the tropical general circulation in the 1990s. *Science*, 295: 838–841.
- Ch eruy, F. and Chevallier, F. (2000). Regional and seasonal variations of the clear sky atmospheric longwave cooling over tropical oceans. *J Clim*, 13: 2863–2875.
- CLIMAP Project Members (1981). Seasonal reconstruction of the Earths surface at the last glacial maximum. Map and Chart Series, 18 pp., Geological Society of America.
- Coakley, J. A. and Baldwin, D. G. (1984). Towards the objective analysis of clouds from imagery data. *J Clim Appl Meteorol*, 23: 1065–1099.
- Del Genio, A. D. and Kovari, W. (2002). Climatic properties of tropical precipitating convection under varying environmental conditions. *J Clim*, 15: 2597–2615.

- Del Genio, A. D., Yao, M.-S., Kovari, W., and Lo, K. K.-W. (1996). A prognostic cloud water parameterization for global climate models. *J Clim*, 9: 270–304.
- Dhuria, H. L. and Kyle, H. L. (1990). Cloud types and the tropical Earth radiation budget. *J Clim*, 3: 1409–1434.
- Emanuel, K. A. (1994). *Atmospheric convection*. Oxford University Press.
- Emanuel, K. A., Neelin, J. D., and Bretherton, C. S. (1994). On large-scale circulations in convecting atmospheres. *Q J R Meteorol Soc*, 120: 1111–1143.
- Emanuel, K. A. and Zivkovic-Rothman, M. (1999). Development and evaluation of a convection scheme for use in climate models. *J Atmos Sci*, 56: 1766–1782.
- Folkins, I. and Braun, C. (2003). Tropical rainfall and boundary layer moist entropy. *J Clim*, 16: 1807–1820.
- Fu, Q., Baker, M., and Hartmann, D. L. (2002). Tropical cirrus and water vapor: An effective Earth infrared iris? *Atmospheric Chemistry and Physics*, 2: 31–37.
- GEWEX Cloud System Science Team (1993). The GEWEX Cloud System Study (GCSS). *Bull Am Meteorol Soc*, 74: 387–389.
- Gibson, J. K., Kallberg, P., Uppala, S., Noumura, A., Hernandez, A., and Serrano, E. (1997). ERA description. ECMWF Re-Analysis Project Report Series, 77 pp., ECMWF, Reading, UK.
- Hartmann, D. L. and Michelsen, M. L. (1993). Large-scale effects on the regulation of tropical sea surface temperature. *J Clim*, 6: 2049–2062.
- Hartmann, D. L., Moy, L. A., and Fu, Q. (2001). Tropical convection and the energy balance at the top of the atmosphere. *J Clim*, 14: 4495–4511.
- Kalnay, E. and co authors (1996). The NCEP/NCAR 40-year reanalysis project. *Bull Am Meteorol Soc*, 77: 437–471.
- Klein, S. A. and Hartmann, D. L. (1993). The seasonal cycle of low stratiform clouds. *J Clim*, 6: 1587–1606.

- Klein, S. A. and Jakob, C. (1999). Validation and sensitivities of frontal clouds simulated by the ECMWF model. *Mon Weather Rev*, 127: 2514–2531.
- Larson, K. and Hartmann, D. L. (2002). Interactions among cloud, water vapor, radiation and large-scale circulation in the tropical climate. Part 2: sensitivity to spatial gradients of sea surface temperature. *J Clim*, page submitted.
- Larson, K., Hartmann, D. L., and Klein, S. A. (1999). The role of clouds, water vapor, circulation, and boundary layer structure in the sensitivity of the tropical climate. *J Clim*, 12: 2359–2374.
- Lau, K.-M., Sui, C. H., Chou, M. D., and Tau, W. K. (1994). An inquiry into the cirrus-thermostat effect for tropical sea surface temperature. *Geophys Res Lett*, 21: 1157–1160.
- Lau, K.-M., Wu, H. T., and Bony, S. (1997). The role of large-scale atmospheric circulation in the relationship between tropical convection and sea surface temperature. *J Clim*, 10: 381–392.
- Le Treut, H. and McAvaney, B. (2000). A model intercomparison of equilibrium climate change in response to CO<sub>2</sub> doubling. Note du Pôle de Modélisation de l’IPSL 18, IPSL, France.
- Levitus, S., Antonov, J. I., Boyer, T. P., and Stephens, C. (2000). Warming of the world ocean. *Science*, 287: 2225–2229.
- Lin, B., Wielicki, B. A., Chambers, L. H., Hu, Y., and Xu, K.-M. (2002). The Iris hypothesis: a negative or positive cloud feedback ? *J Clim*, 15:3–7.
- Lindzen, R. S., Chou, M. D., and Hou, A. Y. (2001). Does the Earth have an adaptive infrared iris? *Bull Am Meteorol Soc*, 82: 417–432.
- Lindzen, R. S. and Nigam, S. (1987). On the role of sea surface temperature gradients in forcing low-level winds and convergence in the tropics. *J Atmos Sci*, 44: 2418–2436.
- Miller, R. L. (1997). Tropical thermostats and low cloud cover. *J Clim*, 10: 409–440.

- Morcrette, J.-J. (1991). Evaluation of model-generated cloudiness: satellite observed and model generated diurnal variability of brightness temperature. *Mon Weather Rev*, 119: 1205–1224.
- Norris, J. R. (1998). Low cloud type over the ocean from surface observations. Part II: geographical and seasonal variations. *J Clim*, 11: 383–403.
- Norris, J. R. and Weaver, C. P. (2001). Improved techniques for evaluating GCM cloudiness applied to the NCAR CCM3. *J Clim*, 14: 2540–2550.
- Pierrehumbert, R. T. (1995). Thermostats, radiator fins, and the local runaway greenhouse. *J Atmos Sci*, 52: 1784–1806.
- Pierrehumbert, R. T. and Roca, R. (1998). Evidence for control of atlantic subtropical humidity by large scale advection. *Geophys Res Lett*, 25: 4537–4540.
- Pope, V. D., Gallani, M. L., Rowntree, P. R., and Stratton, R. A. (2000). The impact of new physical parameterizations in the Hadley Centre climate model. *Clim Dyn*, 16: 123–146.
- Ramanathan, V. and Collins, W. (1991). Thermodynamic regulation of ocean warming by cirrus clouds deduced from observations of the 1987 el-niño. *Nature*, 351: 27–32.
- Salathe, E. and Hartmann, D. L. (1997). A trajectory analysis of tropical upper-tropospheric moisture and convection. *J Clim*, 10: 2533–2547.
- Schubert, S. D., Pfaendtner, J., and Rood, R. (1993). An assimilated dataset for Earth science applications. *Bull Am Meteorol Soc*, 74: 2331–2342.
- Sud, Y. C., Walker, G. K., and Lau, K. M. (1999). Mechanisms regulating sea surface temperatures and deep convection in the tropics. *Geophys Res Lett*, 26: 1019–1022.
- Tompkins, A. M. (2001). On the relationship between tropical convection and sea surface temperature. *J Clim*, 14: 633–637.
- Tompkins, A. M. and Craig, G. C. (1999). Sensitivity of tropical convection to sea surface temperature in the absence of large-scale flow. *J Clim*, 12: 462–476.

- Waliser, D. E. (1996). Formation and limiting mechanism for very high sst: Linking the dynamics and thermodynamics. *J Clim*, 9: 161–188.
- Waliser, D. E. and Graham, N. E. (1993). Convective cloud systems and warm-pool sea surface temperatures: coupled interactions and self-regulation. *J Geophys Res*, 98: 12881–12893.
- Webb, M., Senior, C., Bony, S., and Morcrette, J.-J. (2001). Combining ERBE and ISCCP data to assess clouds in the Hadley Centre, ECMWF and LMD atmospheric climate models. *Clim Dyn*, 17: 905–922.
- Wielicki, B. A., Wong, T., Allan, R. P., Slingo, A., Kiehl, J. T., Soden, B. J., Gordon, C. T., Miller, A. J., Yang, S.-K., Randall, D. A., Robertson, F., Susskind, J., and Jacobowitz, H. (2002). Evidence for large decadal variability in the tropical mean radiative energy budget. *Science*, 295: 841–844.
- Williams, K. D., Ringer, M. A., and Senior, C. A. (2003). Evaluating the cloud response to climate change and current climate variability. *Clim Dyn*, in press.
- Wu, X., Hall, W. D., Grabowski, W. W., Moncrieff, M. W., Collins, W. D., and Kiehl, J. T. (1999). Long-term behavior of cloud systems in TOGA COARE and their interactions with radiative and surface processes. Part II: effects of cloud microphysics on cloud-radiation interaction. *J Atmos Sci*, 56: 3177–3195.
- Wu, X. and Moncrieff, M. W. (1999). Effects of sea surface temperature and large-scale dynamics on the thermodynamic equilibrium state and convection over the tropical western pacific. *J Geophys Res*, 104(D6): 6093–6100.
- Yao, M.-S. and Del Genio, A. D. (2002). Effects of cloud parameterization on the simulation of climate changes in the GISS GCM. Part II: sea surface temperature and cloud feedbacks. *J Clim*, 15: 2491–2503.
- Yin, J. H. and Battisti, D. S. (2001). The importance of tropical sea surface temperature patterns in simulations of last glacial maximum climate. *J Clim*, 14: 565–581.

Yu, W., Doutriaux, M., Sèze, G., Le Treut, H., and Desbois, M. (1996). A methodology study of the validation of clouds in GCMs using ISCCP satellite observations. *Clim Dyn*, 12: 389–401.

## Table Captions

Table 1: Tropically-averaged change in cloud radiative forcing produced in +2 K experiments with the ECMWF, LMD and UKMO GCMs. Units:  $\text{W}/\text{m}^2$ .

Table 2: Decomposition into dynamic, thermodynamic and co-variation components (see equation 3) of the tropically-averaged change in CRF ( $\overline{\delta CRF}$ ) associated with the uniform SST increase of 2 K. Units:  $\text{W}/\text{m}^2$ .

## Figure Captions

Figure 1: Structure of the tropical atmosphere, showing the various regimes, approximately as a function of sea surface temperature (decreasing from left to right) or large-scale vertical velocity in the mid-troposphere (from mean ascending motions on the left to large-scale sinking motions on the right). [*From Emanuel (1994)*].

Figure 2: PDF  $P_\omega$  of the 500 hPa large-scale vertical velocity  $\omega_{500}$  in the Tropics (30°S-30°N) derived from meteorological reanalyses (top) and composite  $C_\omega$  of the ERBE-derived LW CRF in different circulation regimes defined from  $\omega_{500}$  (bottom). Three independent sets of reanalyses are used: the average PDF and LW CRF- $\omega$  relationship are represented by thick lines; vertical bars show the standard deviation of the PDF and of the LW CRF- $\omega$  relationship that results from differences among the reanalysis datasets. The thermodynamic and dynamic components of the CRF response to a climate perturbation arise from a change in  $C_\omega$  (i.e. a change in cloud properties within each individual circulation regime) and  $P_\omega$  (i.e. a change in the statistical weight of the different dynamical regimes), respectively.

Figure 3: Difference, between the +2K and control experiments, of the LW and SW cloud radiative forcing (CRF) and of the 500 hPa vertical velocity ( $w_{500}$ ) simulated by each GCM for December-January-February. The change in SW CRF and in  $w_{500}$  have been multiplied by -1. Units: W/m<sup>2</sup> for CRF changes, hPa/day for  $w_{500}$  changes.

Figure 4: Mean relationships between +2K-CTRL regional monthly anomalies of the tropical CRF (LW, SW) and  $\omega_{500}$  derived from the ECMWF, LMD and UKMO GCMs.

Figure 5: PDF of the 500 hPa vertical velocity over the Tropics (30S-30N) derived from ECMWF, LMD and UKMO GCMs in the CTRL experiment (top), and difference between the PDF of the +2K experiment and that of the CTRL experiment (bottom).

Figure 6: +2K-CTRL change in the LW, SW and NET cloud radiative forcing ( $\delta C_\omega$ ) in each dynamical regime of the Tropics, and effective contribution ( $P_\omega \delta C_\omega$ ) to the tropically-

averaged change in cloud radiative forcing  $\overline{\delta C}$  (note that  $\int_{-\infty}^{+\infty} P_{\omega} \delta C_{\omega} d\omega$  equals the thermodynamic component of  $\overline{\delta C}$  reported in Table 2).

Figure 7: Composites  $C_{\omega}$  of the mean LW, SW and NET cloud radiative forcing in different dynamical regimes defined from the monthly mean 500 hPa vertical velocity. For each dynamical regime are reported the composites derived from GCM simulations (color bars) as well as composites derived from ERBE data for the cloud radiative forcing and different sets of atmospheric reanalyses for the 500 hPa vertical velocity (white bars, ERA, NCEP/NCAR or NASA/DAO from left to right). Units are in  $\text{W}/\text{m}^2$ .

Figure 8: For the ECMWF, LMD and UKMO GCMs: mean relationship between the 500 hPa vertical motion (negative values indicate large-scale ascent) and the SST (top) over tropical oceans for the CTRL simulation (in blue) and the +2K experiment (in red). Vertical bars represent the standard deviation around the mean. Middle: Same relationship but expressed as a function of the SST minus the tropically-averaged SST. Bottom: Frequency of occurrence of large-scale rising motion situations (negative monthly mean value of  $\omega_{500}$  computed for SST intervals of 1 K) expressed as a function of the SST minus the tropically-averaged SST. Are reported only the bins for which the number of points exceeds 1% of the total number of points over tropical oceans.

Figure 9: Sketch of idealized numerical experiments that may be performed by single-column models or cloud-resolving models to investigate the physical processes that control the sensitivity of cloud properties to a change in the large-scale atmospheric vertical motion on the one hand (left), and to a change in the thermodynamic structure of the atmosphere (e.g. resulting from a change in the carbon dioxide concentration in the atmosphere) on the other hand (right).

	ECMWF	LMD	UKMO
$\overline{\delta C_{net}}$	-1.80	0.85	2.02
$\overline{\delta C_{sw}}$	-1.34	0.18	1.81
$\overline{\delta C_{lw}}$	-0.46	0.67	0.22

Table 1: Tropically-averaged change in cloud radiative forcing produced in +2 K experiments with the ECMWF, LMD and UKMO GCMs. Units: W/m<sup>2</sup>.

		ECMWF	LMD	UKMO
$\overline{\delta C_{net}}$	total	-1.80	0.85	2.02
	dynamic	0.10	-0.05	-0.03
	thermodynamic	-1.90	0.93	2.09
	co-variation	0.0	-0.03	-0.04
$\overline{\delta C_{sw}}$	total	-1.34	0.18	1.81
	dynamic	0.29	0.06	0.22
	thermodynamic	-1.67	0.13	1.59
	co-variation	0.05	-0.01	-0.01
$\overline{\delta C_{lw}}$	total	-0.46	0.67	0.22
	dynamic	-0.19	-0.11	-0.25
	thermodynamic	-0.22	0.80	0.50
	co-variation	-0.05	-0.02	-0.03

Table 2: Decomposition into dynamic, thermodynamic and co-variation components (see equation 3) of the tropically-averaged change in CRF ( $\overline{\delta CRF}$ ) associated with the uniform SST increase of 2 K. Units: W/m<sup>2</sup>.

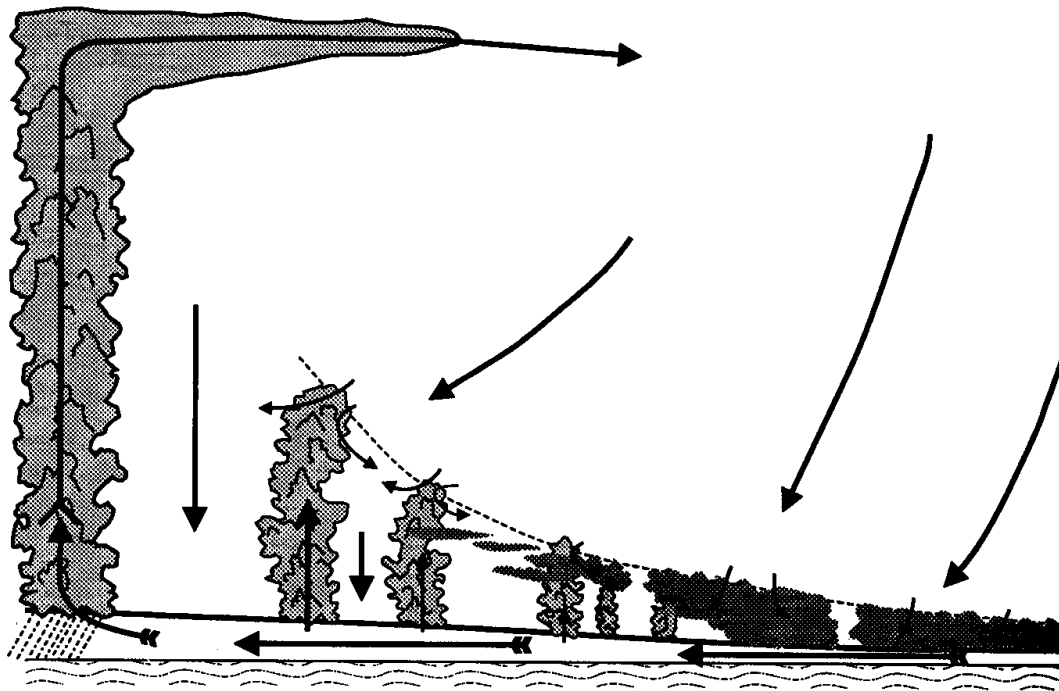


Figure 1: Structure of the tropical atmosphere, showing the various regimes, approximately as a function of sea surface temperature (decreasing from left to right) or large-scale vertical velocity in the mid-troposphere (from mean ascending motions on the left to large-scale sinking motions on the right). [From Emanuel (1994).]

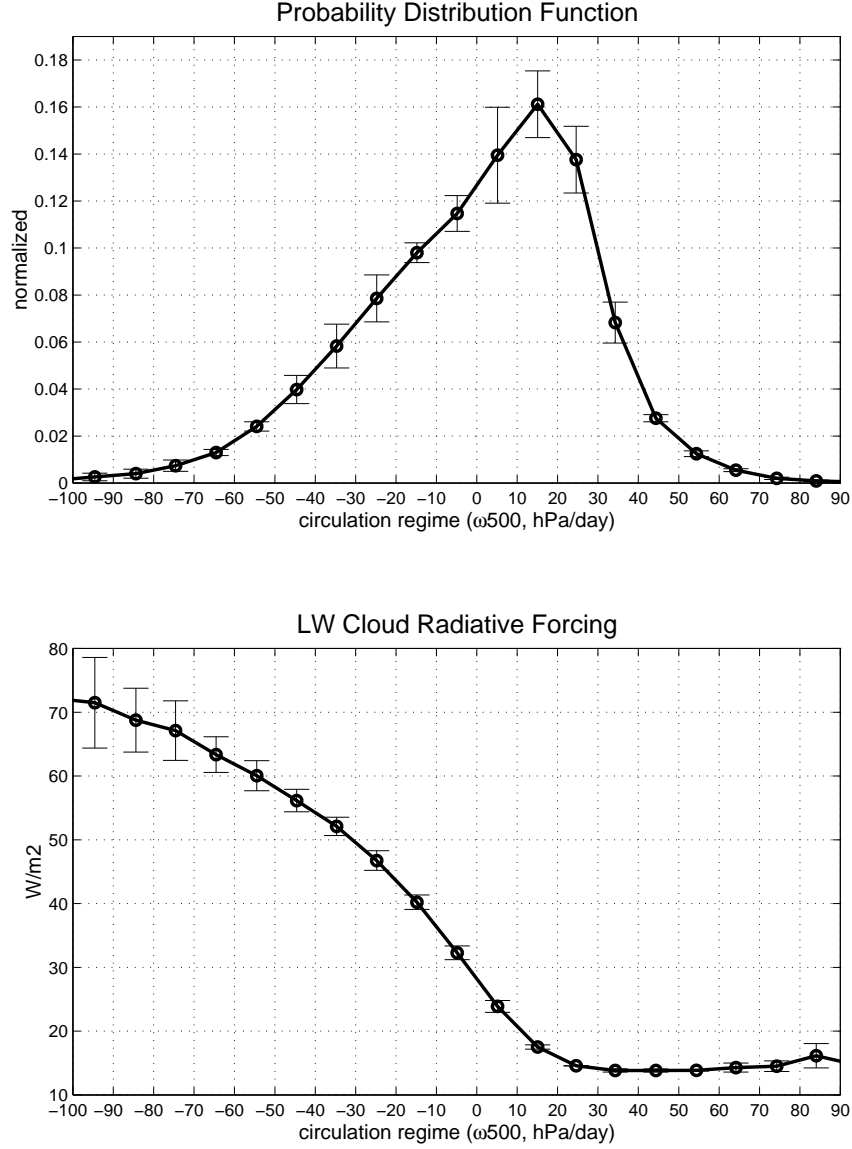


Figure 2: PDF  $P_\omega$  of the 500 hPa large-scale vertical velocity  $\omega_{500}$  in the Tropics ( $30^\circ\text{S}$ - $30^\circ\text{N}$ ) derived from meteorological reanalyses (top) and composite  $C_\omega$  of the ERBE-derived LW CRF in different circulation regimes defined from  $\omega_{500}$  (bottom). Three independent sets of reanalyses are used: the average PDF and LW CRF- $\omega$  relationship are represented by thick lines; vertical bars show the standard deviation of the PDF and of the LW CRF- $\omega$  relationship that results from differences among the reanalysis datasets. The thermodynamic and dynamic components of the CRF response to a climate perturbation arise from a change in

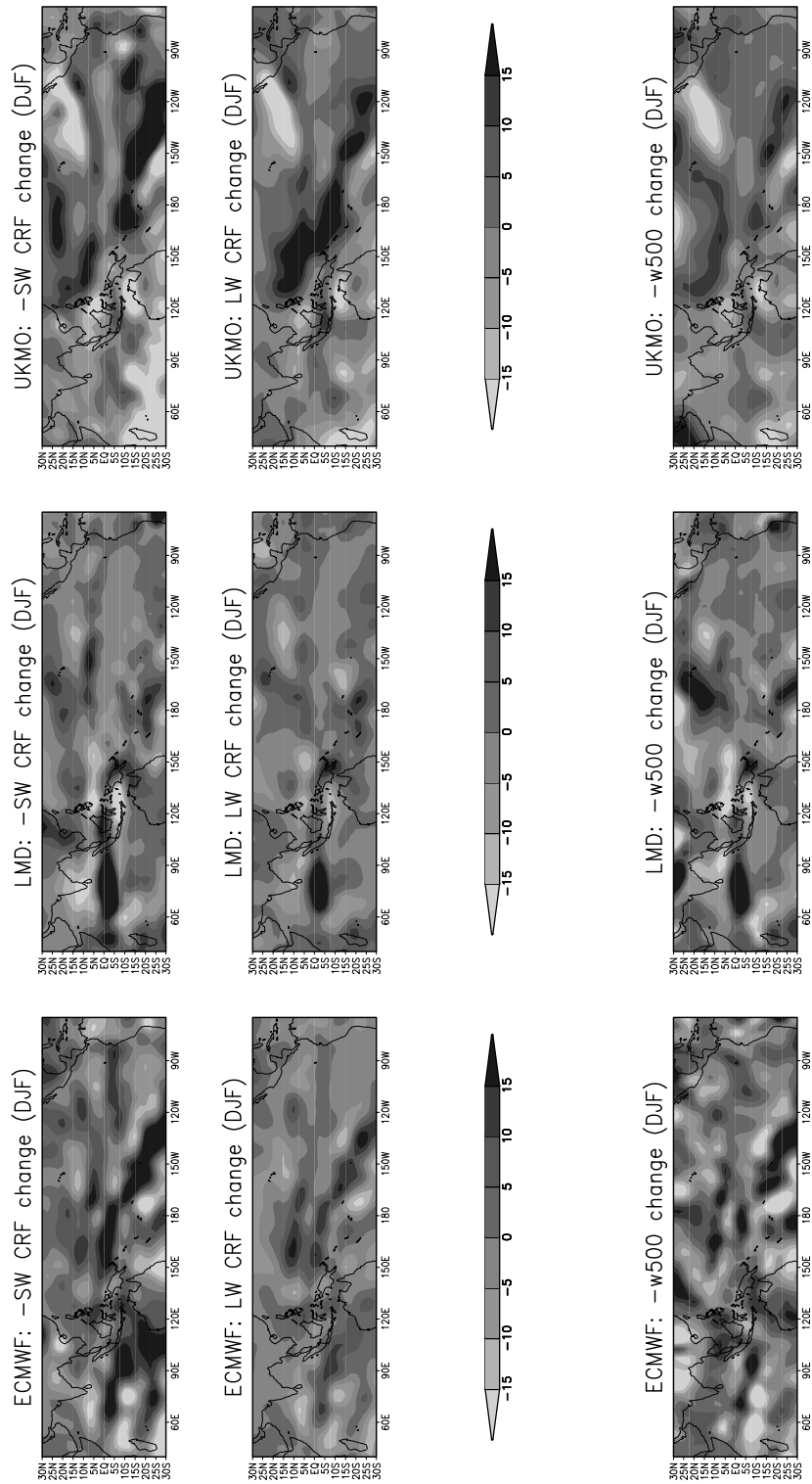


Figure 3: Difference, between the +2K and control experiments, of the LW and SW cloud radiative forcing (CRF) and of the 500 hPa vertical velocity (w500) simulated by each GCM for December-January-February. The change in SW CRF and in w500 have been multiplied

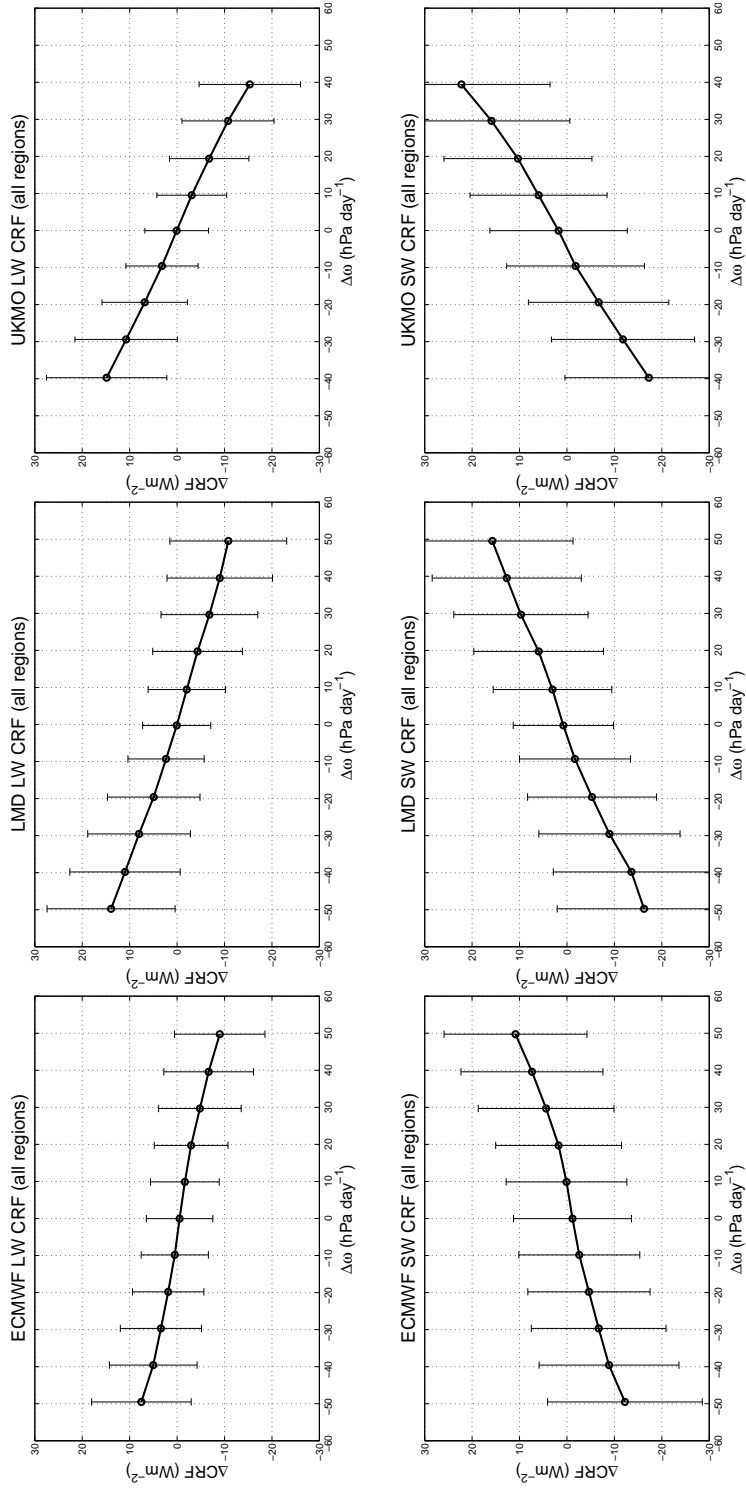


Figure 4: Mean relationships between +2K-CTRL regional monthly anomalies of the tropical CRF (LW, SW) and  $\omega_{500}$  derived from the ECMWF, LMD and UKMO GCMs.

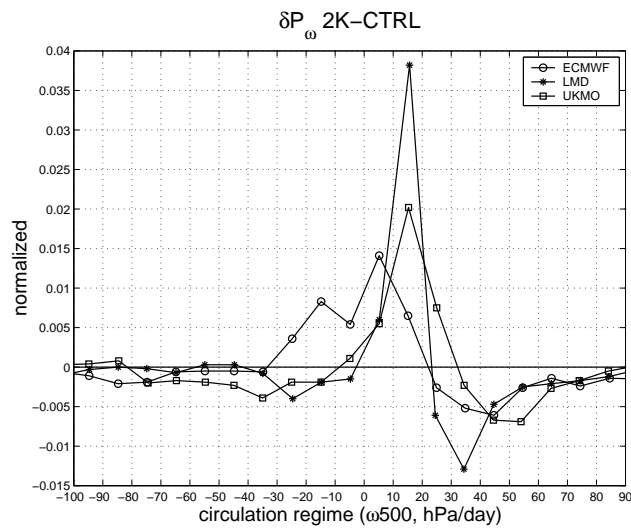
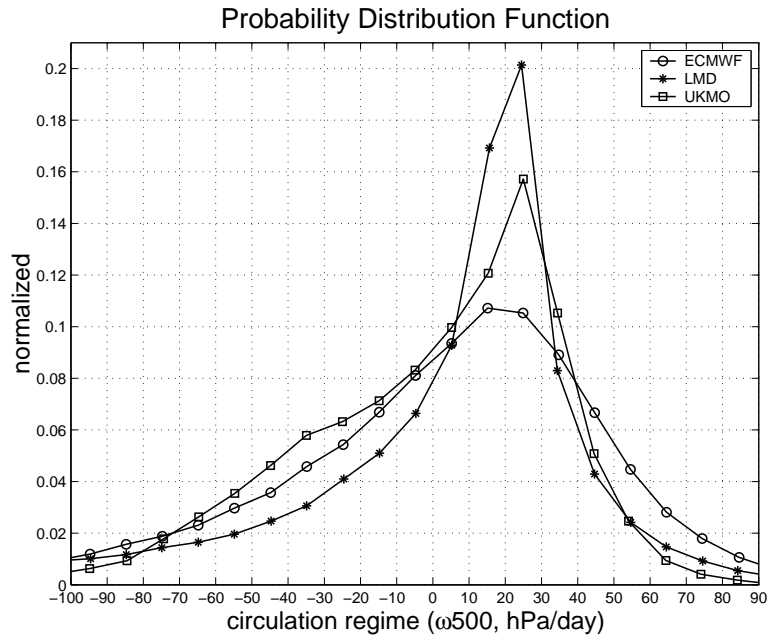


Figure 5: PDF of the 500 hPa vertical velocity over the Tropics (30S-30N) derived from ECMWF, LMD and UKMO GCMs in the CTRL experiment (top), and difference between the PDF of the +2K experiment and that of the CTRL experiment (bottom).

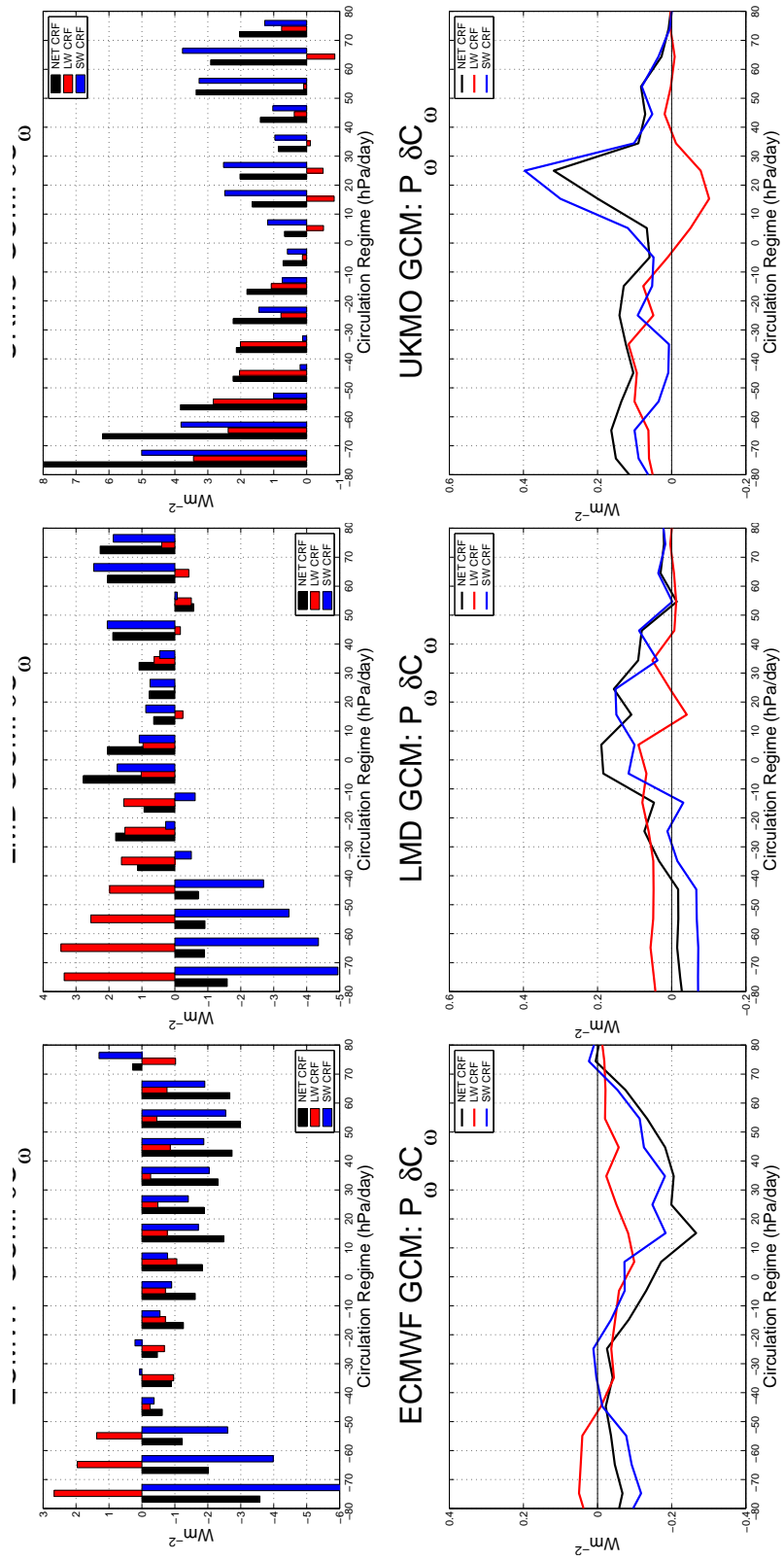


Figure 6: +2K-CTRL change in the LW, SW and NET cloud radiative forcing ( $\delta C_\omega$ ) in each dynamical regime of the Tropics, and effective contribution ( $P_\omega \delta C_\omega$ ) to the tropically-averaged change in cloud radiative forcing  $\overline{\delta C}$  (note that  $\int_{-\infty}^{+\infty} P_\omega \delta C_\omega d\omega$  equals the thermo-

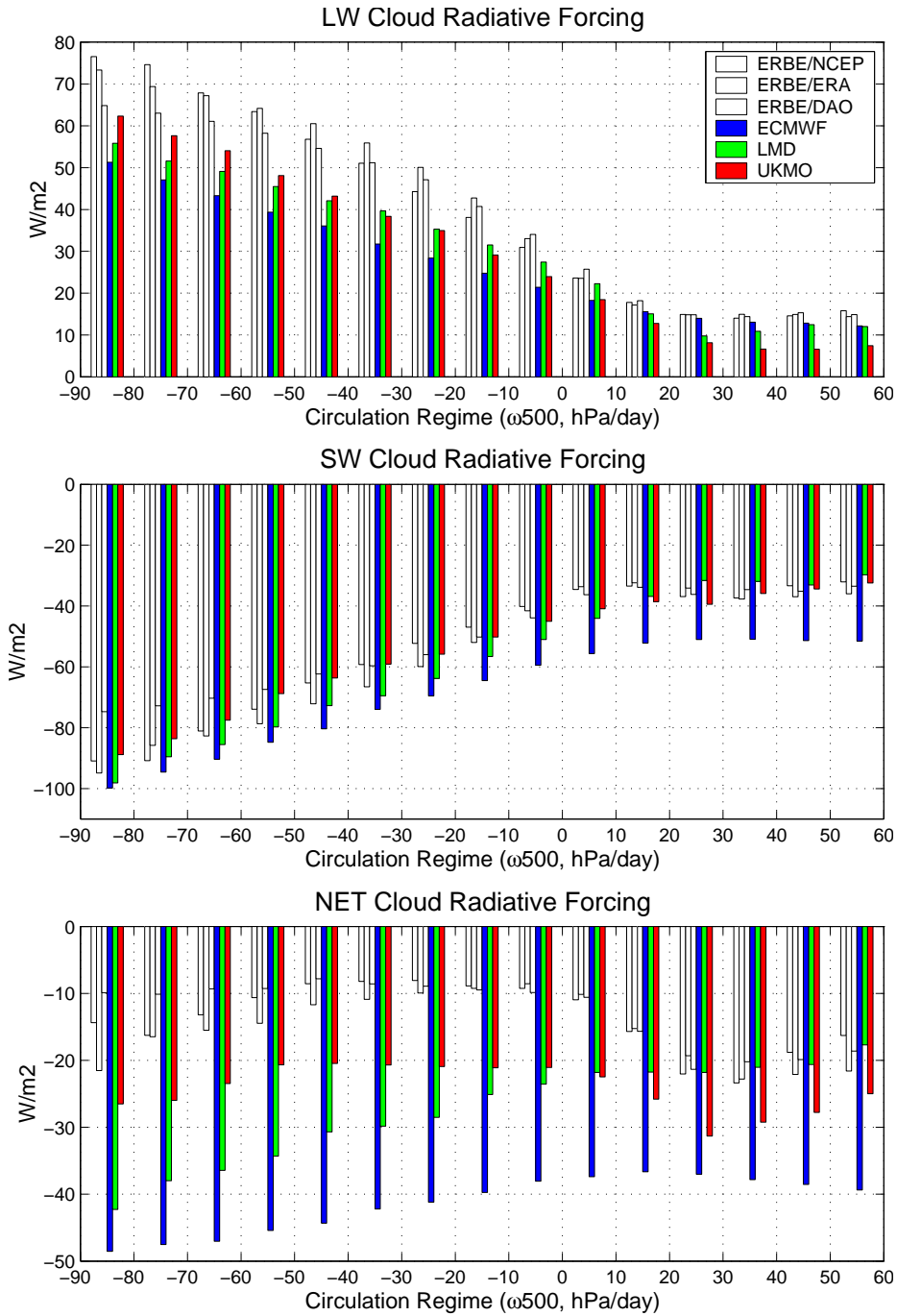


Figure 7: Composites  $C_\omega$  of the mean LW, SW and NET cloud radiative forcing in different dynamical regimes defined from the monthly mean 500 hPa vertical velocity. For each dynamical regime are reported the composites derived from GCM simulations (color bars) as well as composites derived from ERBE data for the cloud radiative forcing and different sets of atmospheric reanalyses for the 500 hPa vertical velocity (white bars, ERA, NCEP/NCAR or NASA/DAO from left to right). Units are in  $W/m^2$ .

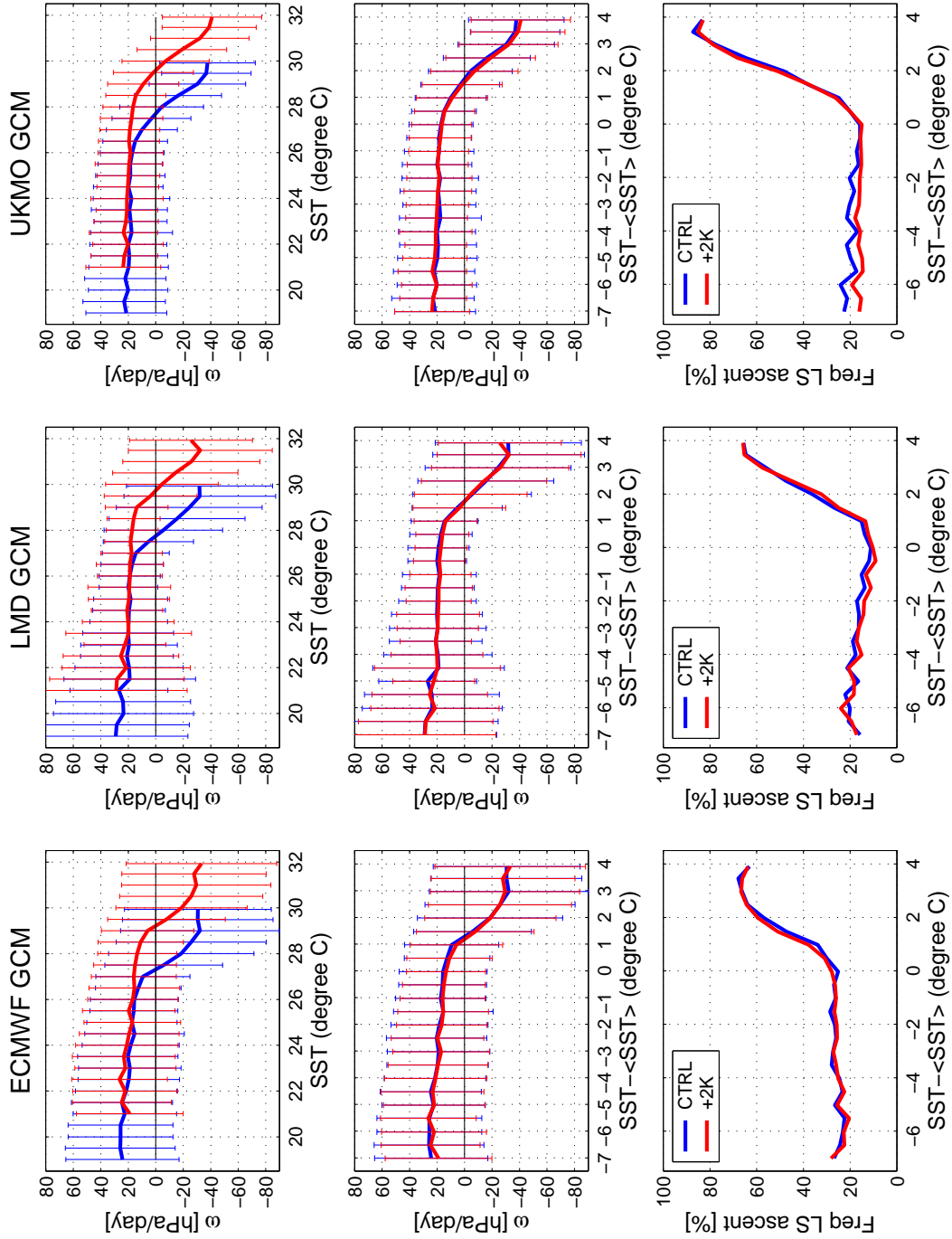


Figure 8: For the ECMWF, LMD and UKMO GCMs: mean relationship between the 500 hPa vertical motion (negative values indicate large-scale ascent) and the SST (top) over tropical oceans for the CTRL simulation (in blue) and the +2K experiment (in red). Vertical bars represent the standard deviation around the mean. Middle: Same relationship but expressed as a function of the SST minus the tropically-averaged SST. Bottom: Frequency of occurrence of large-scale rising motion situations (negative monthly mean value of  $\omega_{500}$  computed for SST intervals of 1 K) expressed as a function of the SST minus the tropically-

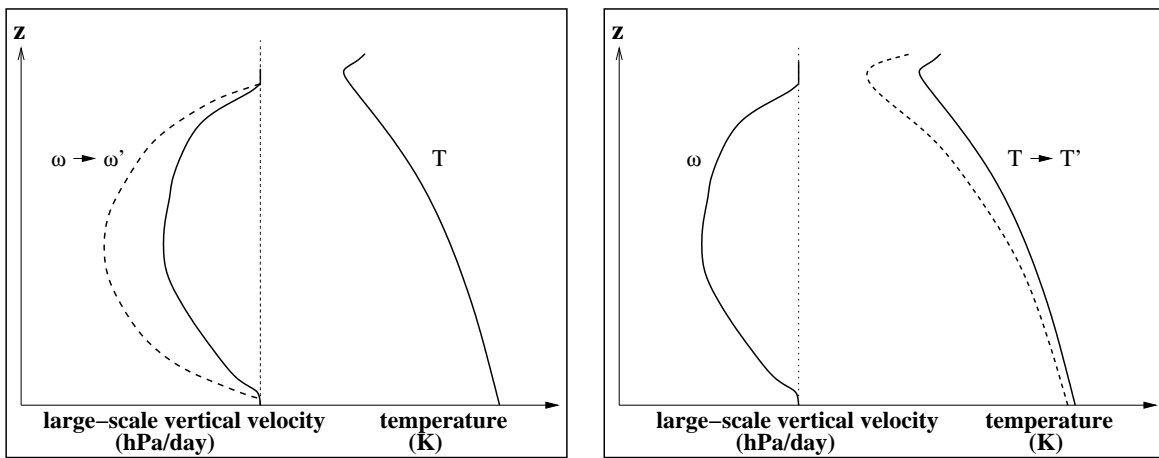


Figure 9: Sketch of idealized numerical experiments that may be performed by single-column models or cloud-resolving models to investigate the physical processes that control the sensitivity of cloud properties to a change in the large-scale atmospheric vertical motion on the one hand (left), and to a change in the thermodynamic structure of the atmosphere (e.g. resulting from a change in the carbon dioxide concentration in the atmosphere) on the other hand (right).